Nanoscale Transformations in Steels

J. Millan, D. Ponge, L. Yuan, S. Sandlöbes, M. Kuzmina, S. Goto, Y. Li, P. Choi, S. Zaefferer, A. Nematollahi, M. Herbig, J. Wittig, R. Kirchheim, G. Inden, J. Neugebauer, D. Raabe

shortened version

Max-Planck-Institut
für Eisenforschung GmbH
Düsseldorf, Germany

WWW.MPIE.DE
d.raabe@mpie.de

MDP 2013

13-16, April 2013
Shenyang, China

Workshop on Microstructure-driven Design & Performance of Advanced Metals

High strength plus high ductility: strain hardening at high strains

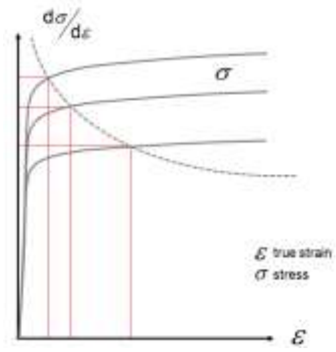

Inverse strength-ductility relation

Delayed onset of hardening:

Twins, martensite, dislocation substructures, gradual phase dissolution,…

Permanent strain hardening

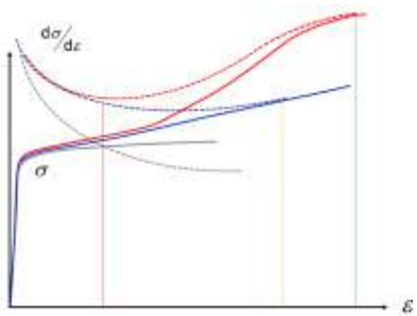

Design strain hardening only where needed

Examples

Pearlite: the limits of strength

Nano-austenite reversion

Fe-based superalloy

~7 GPa

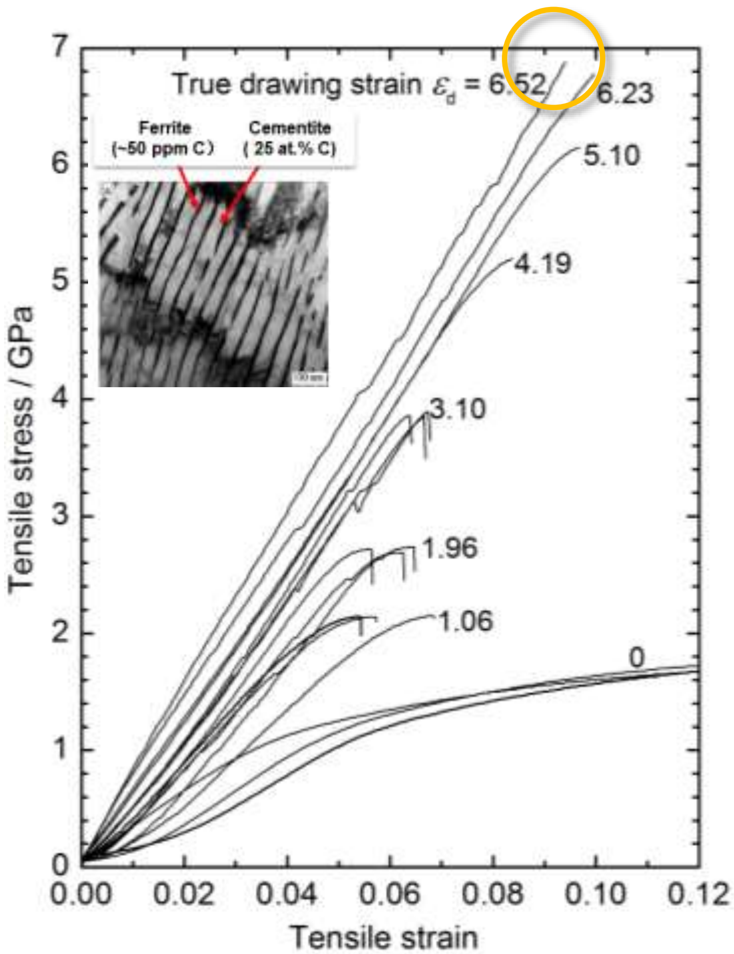
True drawing strain ε_d = 6.52
6.23
5.10
4.19
3.10
1.96
1.06
0
Ferrite
(~50 ppm C)
Cementite
(25 at.% C)
Tensile stress / GPa
Tensile strain
0.00
0.02
0.04
0.06
0.08
0.10
0.12
0
1
2
3
4
5
6
7

Towards the limits of strength: cold-drawn pearlitic steel

Ferrite (~50 ppm C) **Cementite (25 at.% C)**

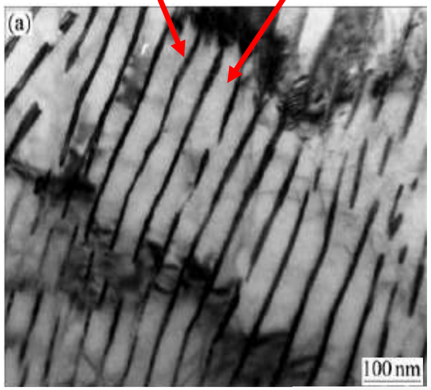

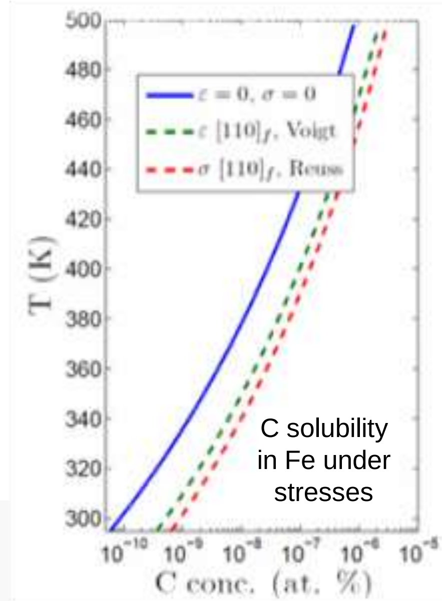

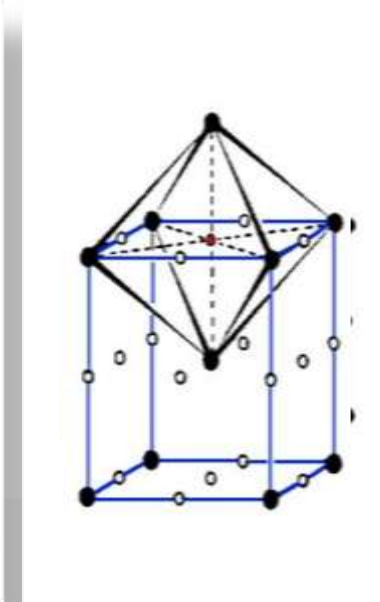

; = 2)

ale: nm

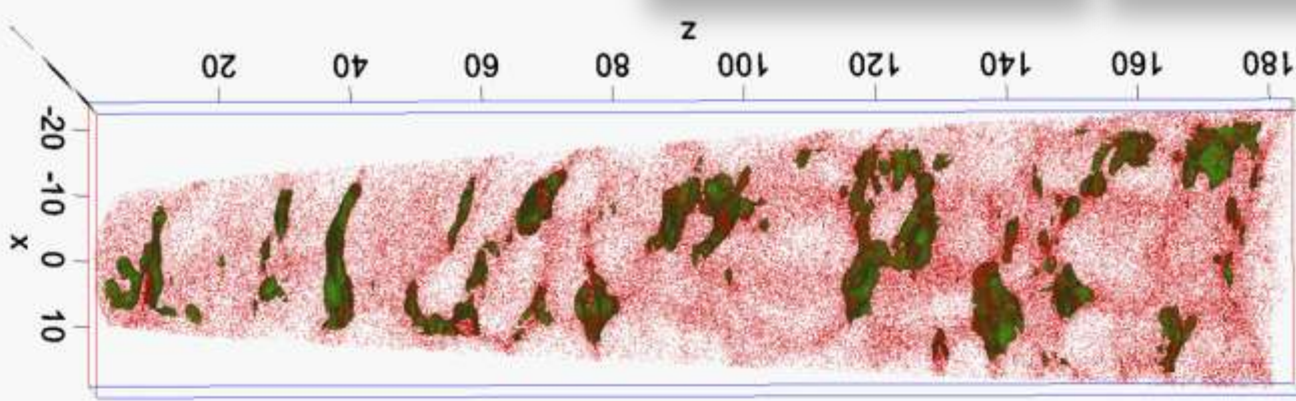

C iso-concentration (7 at.%)

• C

(ε = 6.5)

Examples

Pearlite: the limits of strength

Nano-austenite reversion

Fe-based superalloy

Segregation Engineering: nanostructuring by transformation

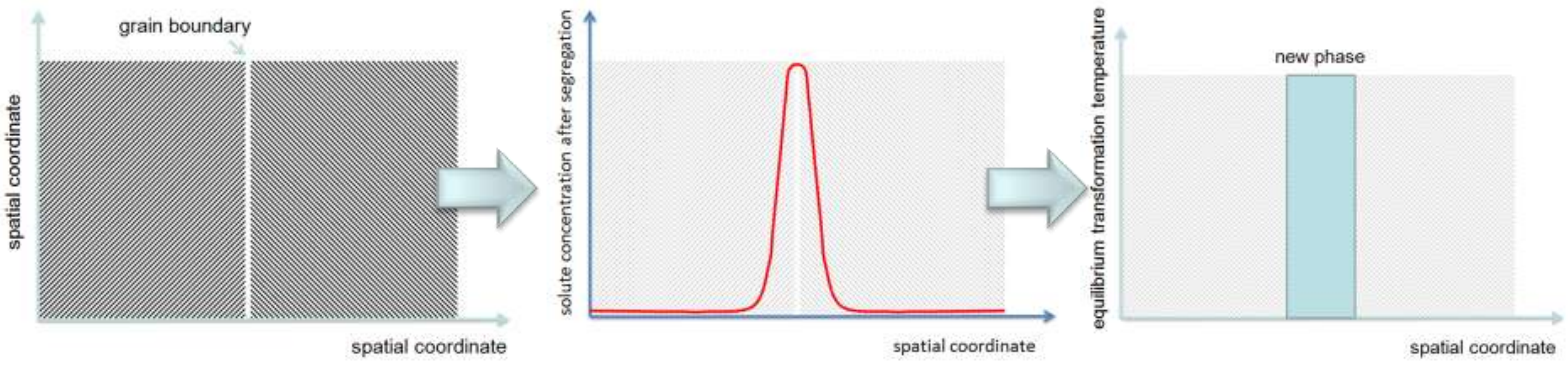

Solute segregation to martensite grain boundaries

Local phase transformation at grain boundary
(martensite-to-austenite reversion confined to GB)

Self-organized nanostructuring by selective phase transformation

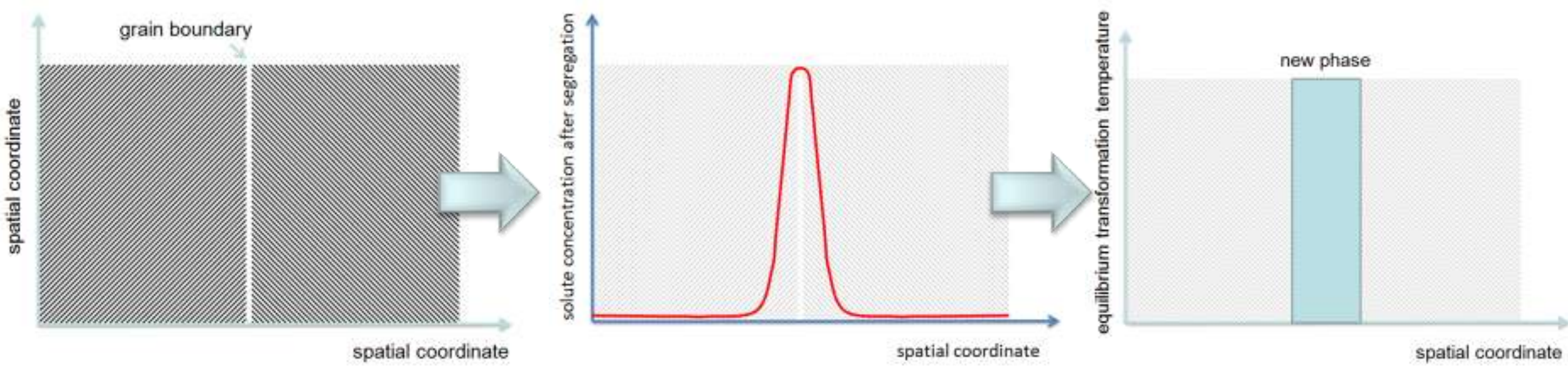

Solute segregation to martensite grain boundaries

- Element with high segregation tendency
- Reduce transformation temperature (e.g. from martensite to austenite)
- Prefer segregation over bulk precipitation (e.g. carbide)

Local phase transformation at grain boundary (martensite-to-austenite reversion confined to GB)

Mn segregation at grain boundary, (450°C/65h)

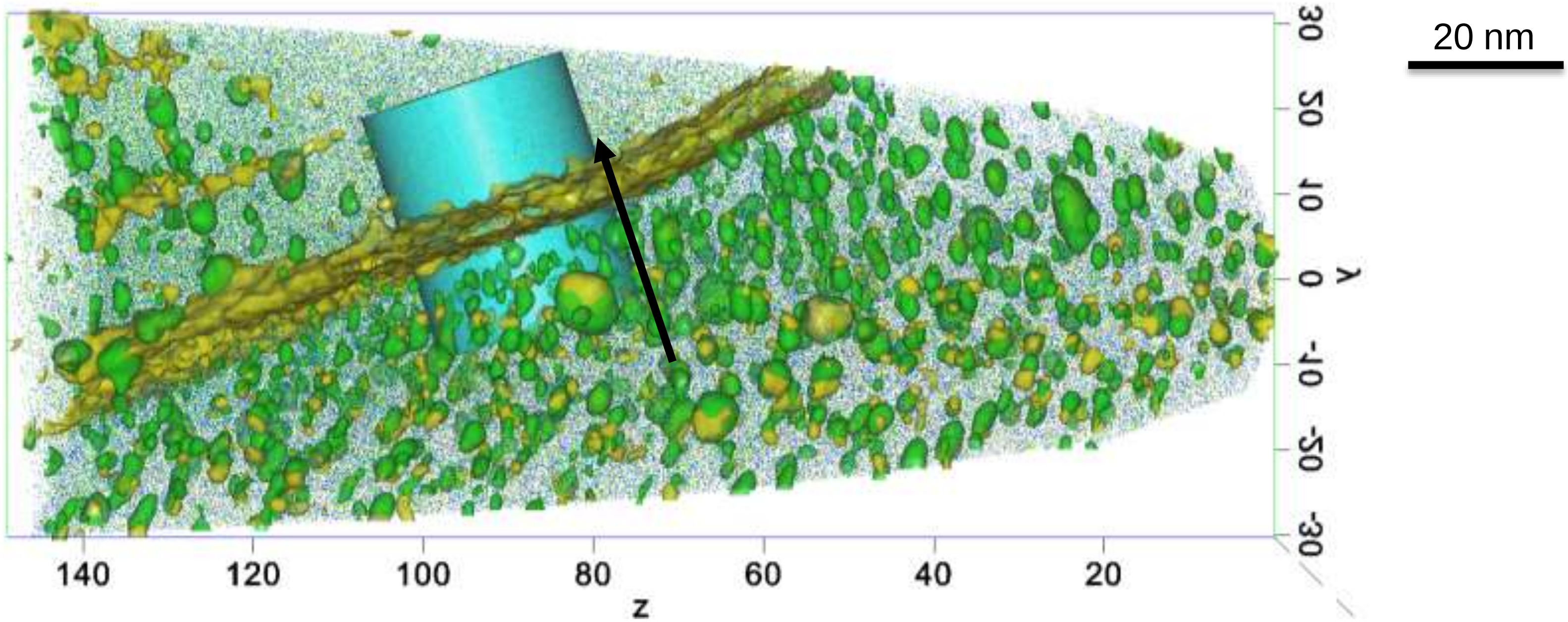

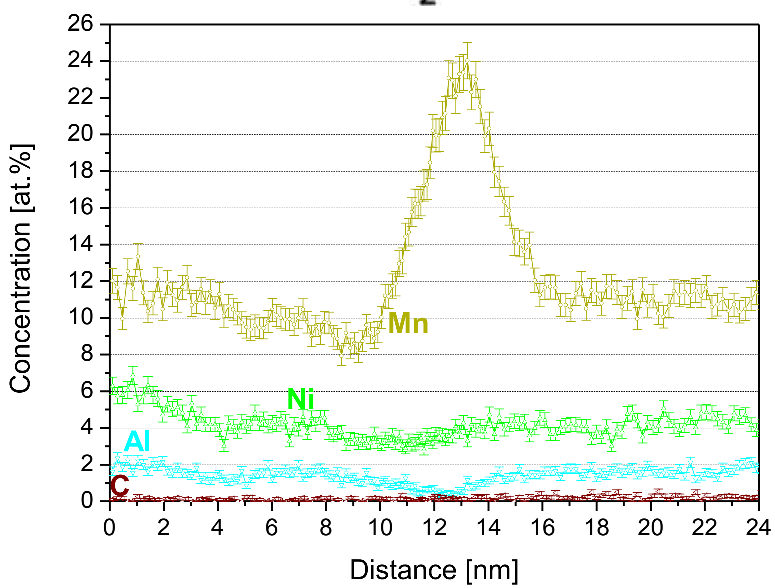

9Mn-2Ni-0.15Al-1Ti-1Mo (wt.%)

9Mn-2Ni-0.15Al-1Ti-1Mo (wt.%), aged 450°C/65h

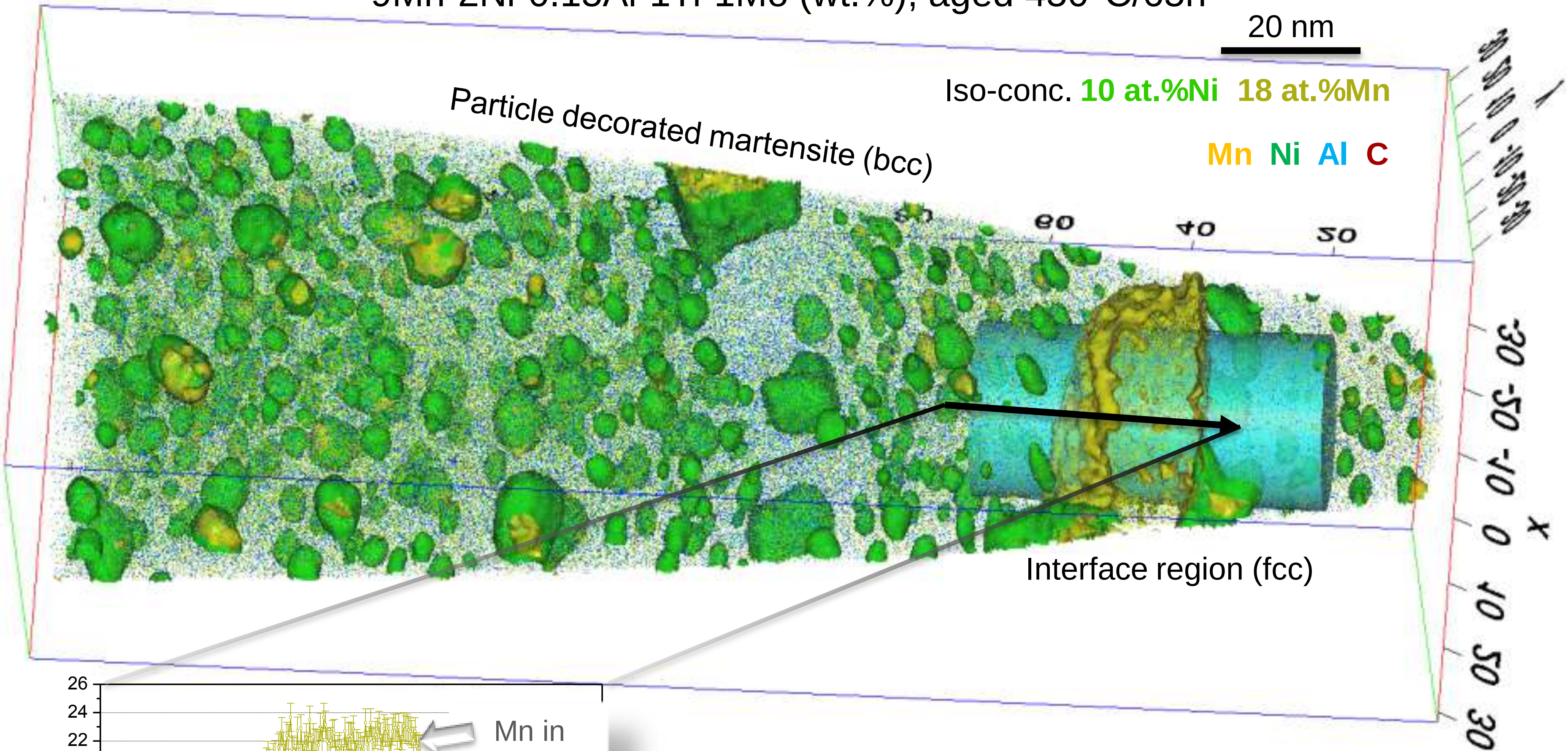

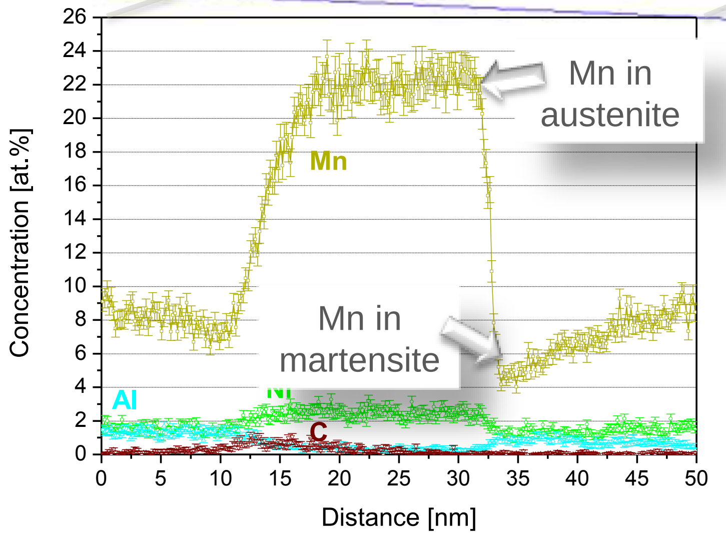

Phase formation at martensite interface
Near-equilibrium partitioning at interface

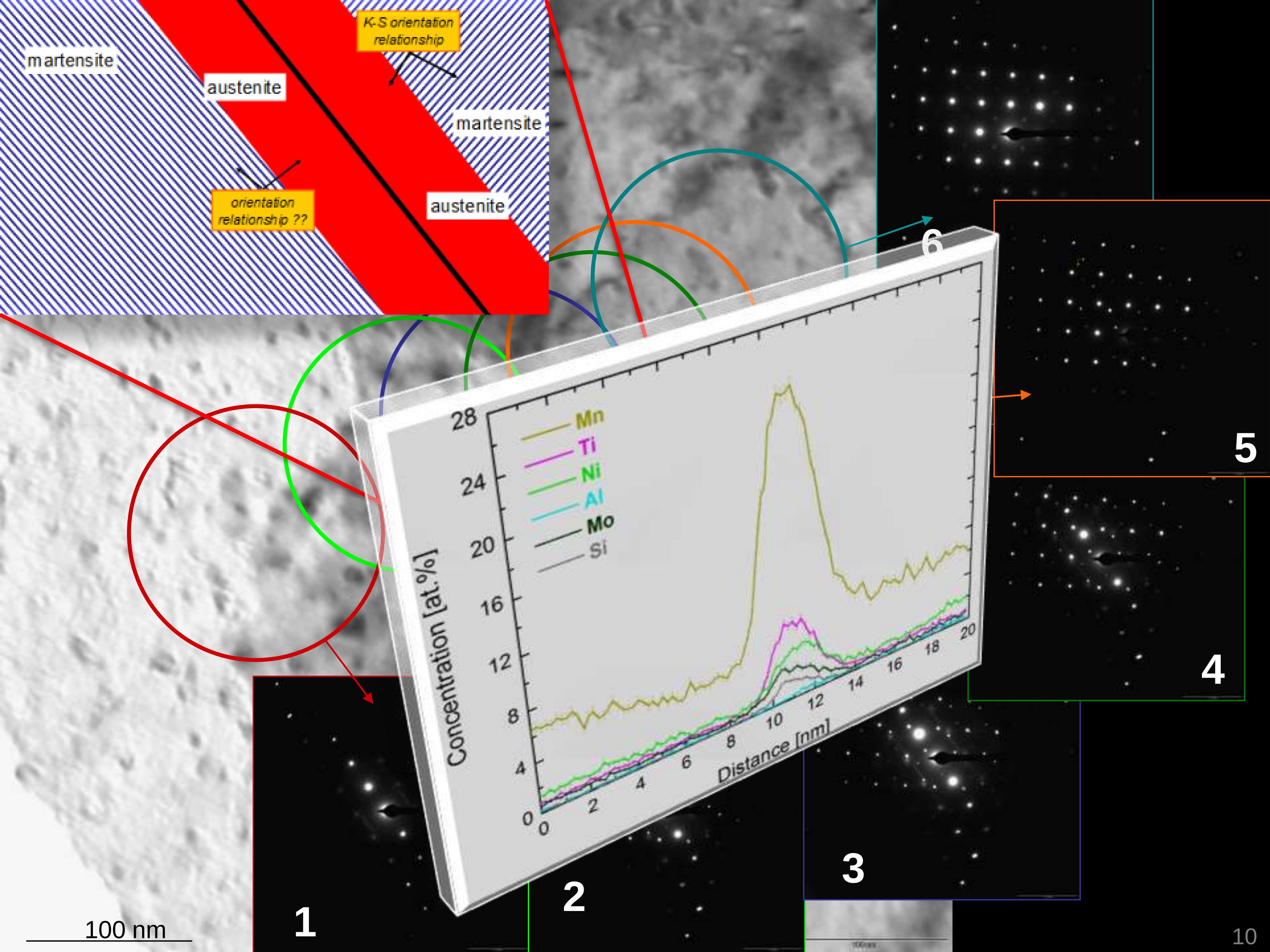

martensite
austenite
K-S orientation relationship
martensite
orientation relationship ??
austenite
Mn
Ti
Ni
Al
Mo
Si
Concentration [at.%]
Distance [nm]
1
2
3
4
5
6
100 nm

Thin intergranular FCC layer among two martensite crystals, APT

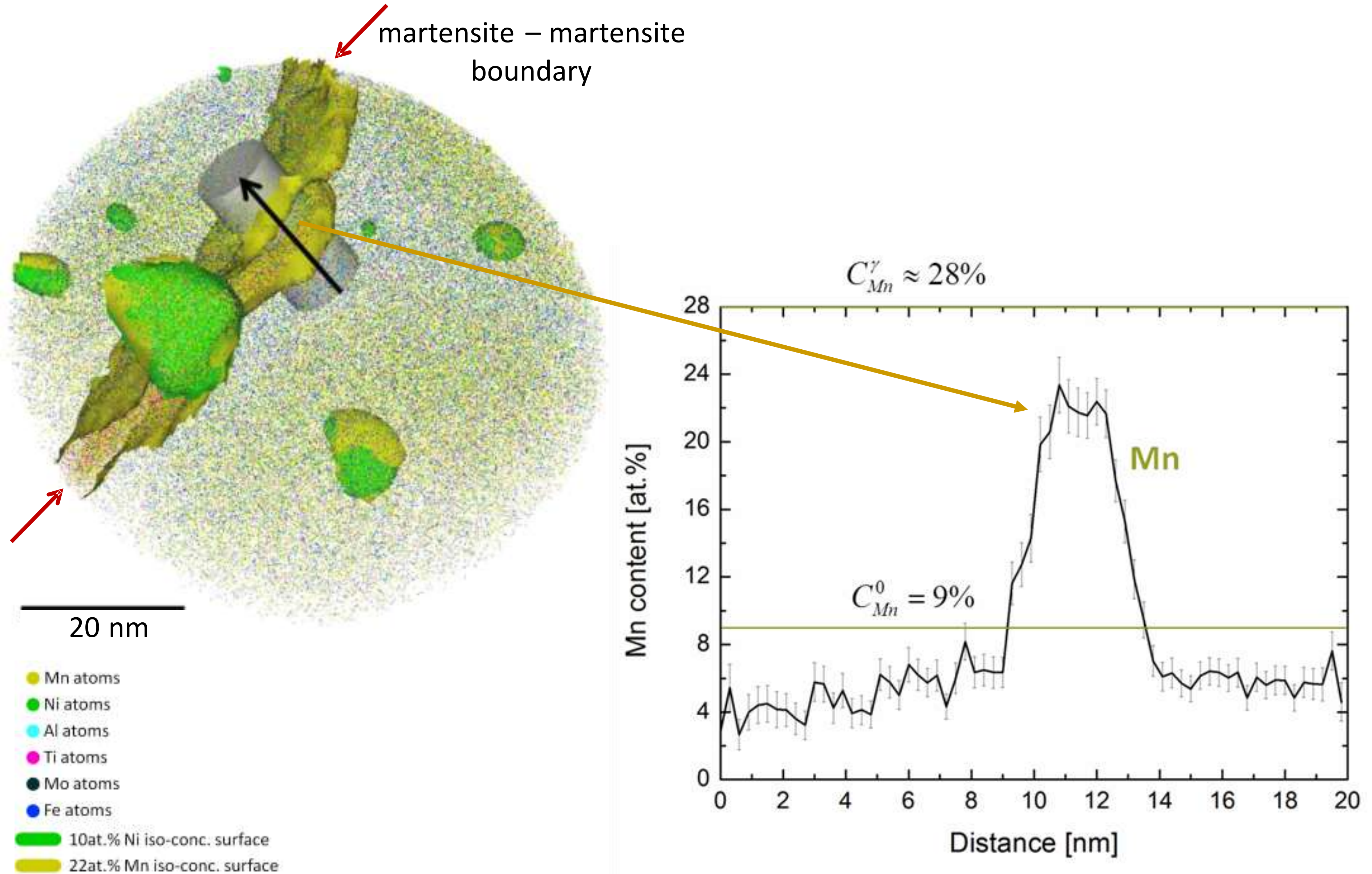

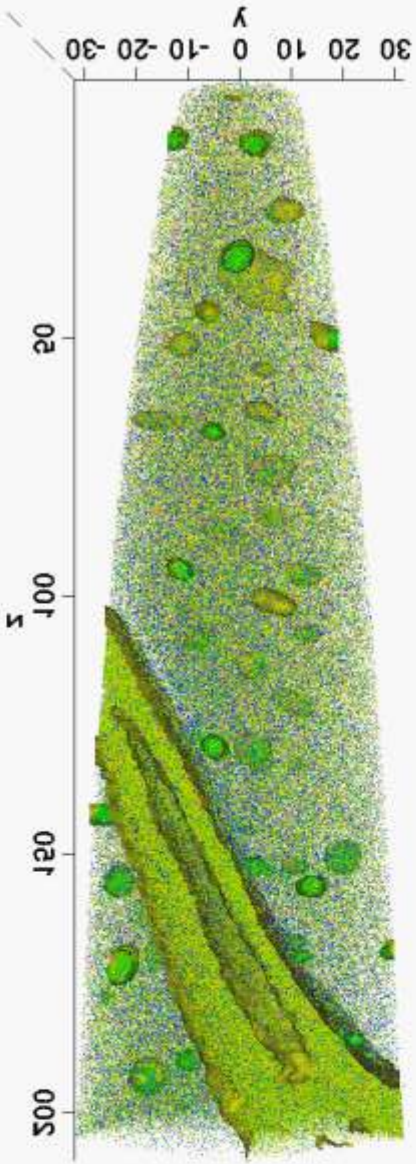

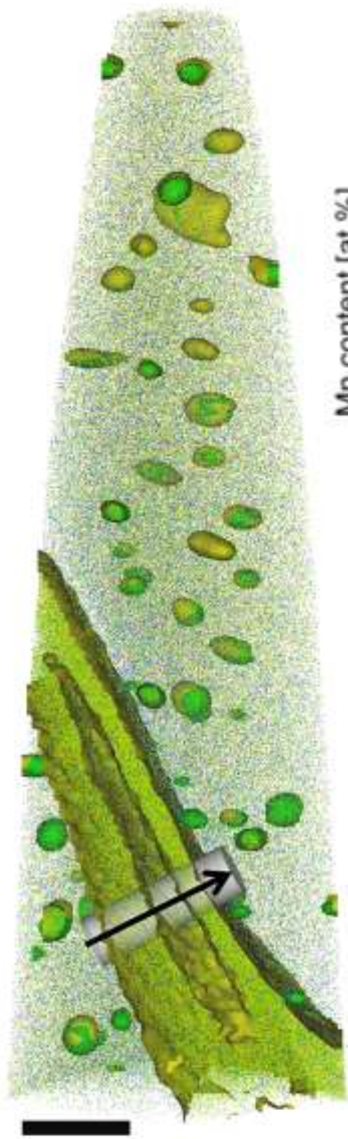

Mn profile

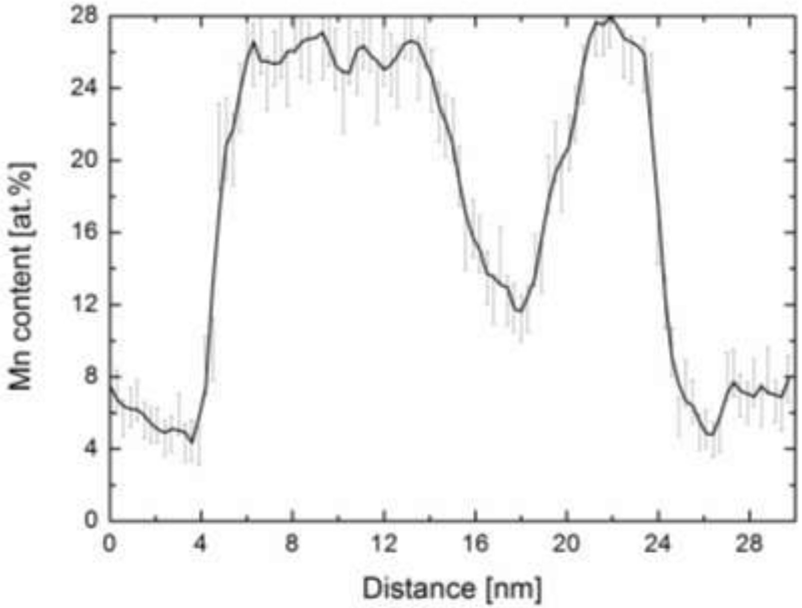

C	Ni	Mo	Ti	Al	Mn	Fe
0.01	2.0	1.0	1.0	0.15	12	bal.

650 MPa to 2 GPa

Making martensite ductile

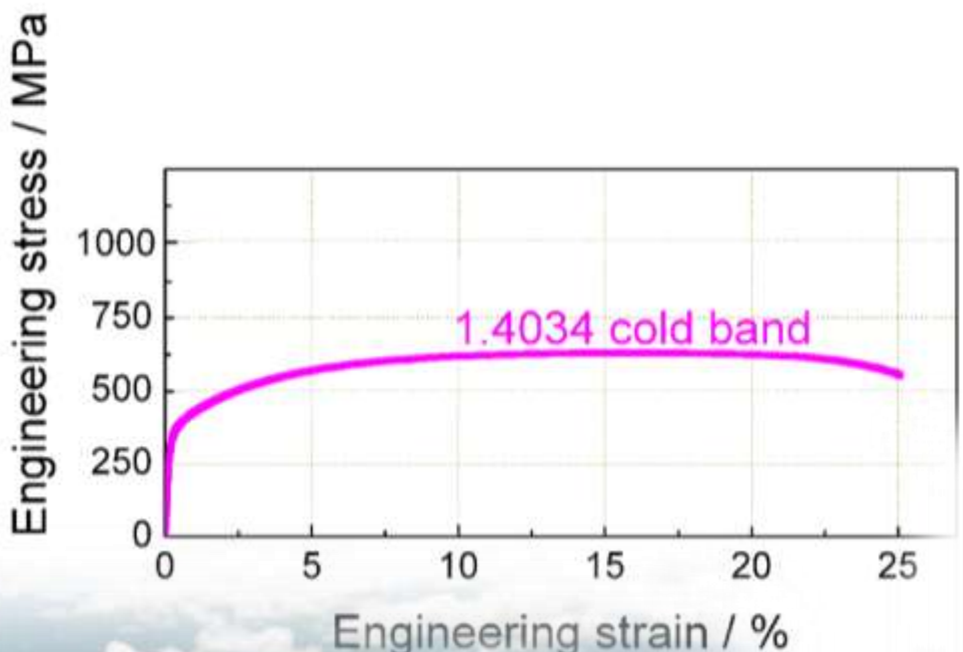

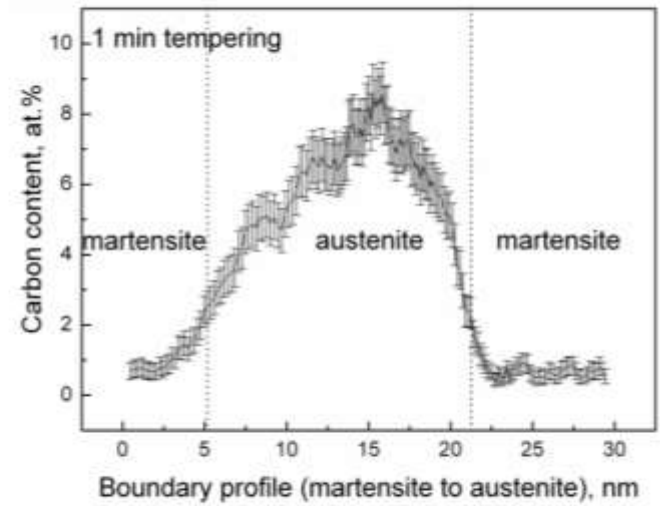

Fe-13.6Cr-0.44C (wt.%)

Pearlite: the limits of strength

Nano-austenite reversion

Fe-based superalloy

Fe-Mn steel, weight reduced (10% less mass density)

κ-carbide (iso-surface of 9 at.% C)

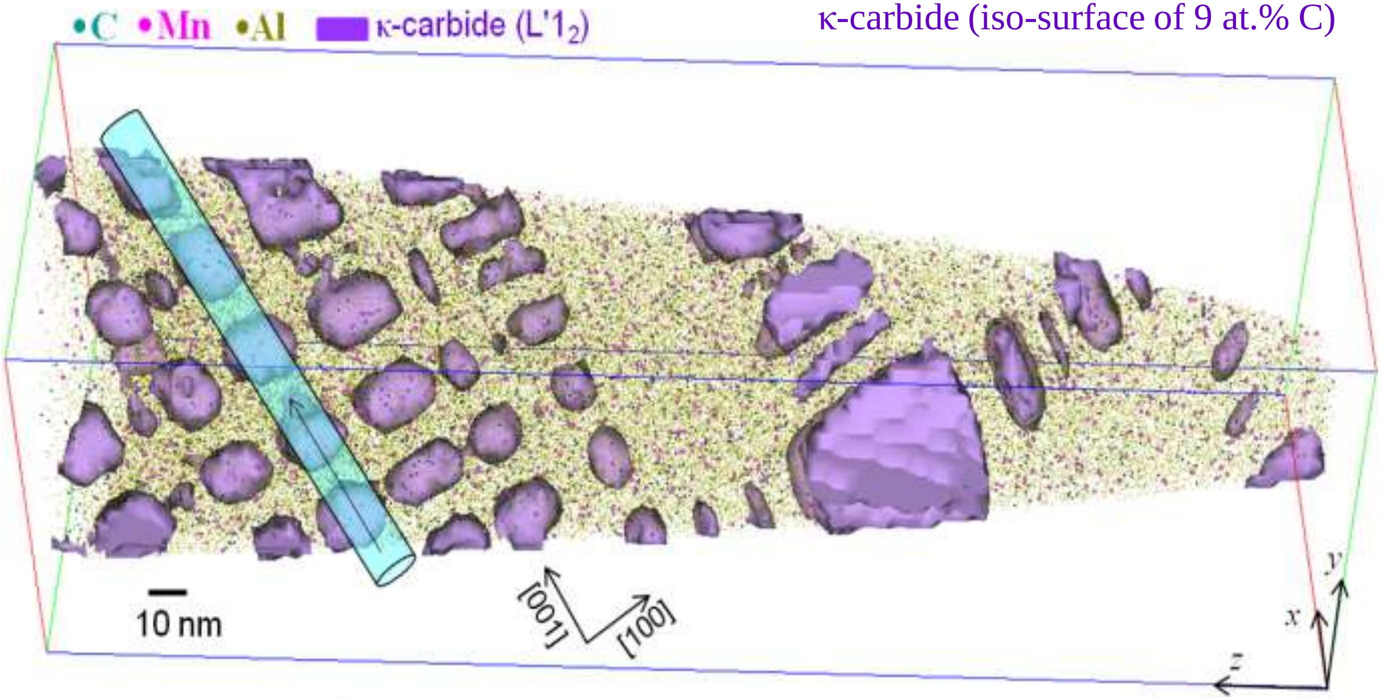

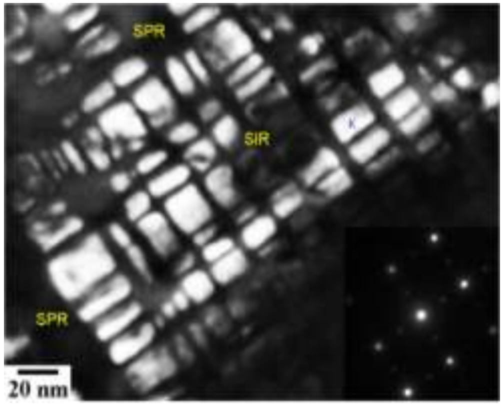

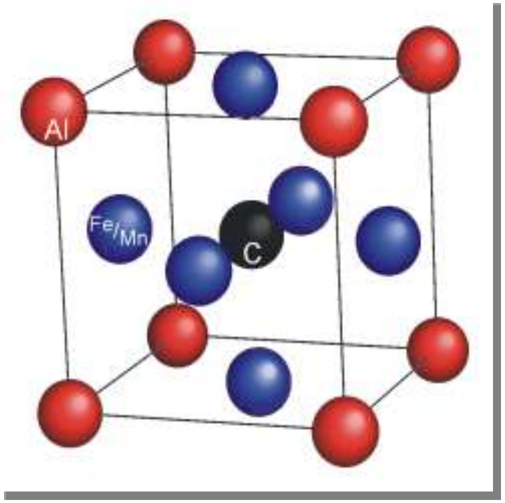

Lattice structure
of κ-Carbides,
Perowskite type

Conclusions

- Design alloys by self-organized nanostructuring
- Segregation plus confined phase transformation at defects
- Works for dislocations too?
- Deformation-driven mechanical bulk alloying leads to non-equilibrium phases approaching the theoretical limits of strength
- Designing stable nanocarbides enables weight-reduced ultra-ductile and thermally stable materials

References

O. Dmitrieva, D. Ponge, G. Inden, J. Millán, P. Choi, J. Sietsma, D. Raabe: Acta Materialia 59 (2011) 364-374, DOI: 10.1016/j.actamat.2010.09.042
Chemical gradients across phase boundaries between martensite and austenite in steel studied by atom probe tomography and simulation

E.A. Marquis, P.-Pa Choi, F. Danoix, K. Kruska, S. Lozano-Perez, D. Ponge, D. Raabe, and C.A. Williams: MICROSCOPY TODAY 20(4) 44-48 (2012)
New Insights Into The Atomic-Scale Structures And Behavior Of Steels

Y.J. Li, P. Choi, S. Goto, C. Borchers, D. Raabe, R. Kirchheim: Acta Materialia, Volume 60, Issue 9, May 2012, Pages 4005-4016
Evolution of strength and microstructure during annealing of heavily cold-drawn 6.3 GPa hypereutectoid pearlitic steel wire

D. Raabe, P. P. Choi, Y.J. Li, A. Kostka, X. Sauvage, F. Lecouturier, K. Hono, R. Kirchheim, R. Pippan, D. Embury: MRS Bulletin 35 (2010) 982-991
Metallic composites processed via extreme deformation: Toward the limits of strength in bulk materials

Y.J. Li, P.P. Choi, C. Borchers, S. Westerkamp, S. Goto, D. Raabe, R. Kirchheim: Acta Materialia 59 (2011) 3965–3977
Atomic-scale mechanisms of deformation-induced cementite decomposition in pearlite

D. R. Steinmetz, T. Jäpel, B. Wietbrock, P. Eisenlohr, I. Gutierrez-Urrutia, A. Saeed-Akbari, T. Hickel, F. Roters, D. Raabe: Acta Materialia 61 (2013) 494-510
Revealing the strain-hardening behavior of twinning-induced plasticity steels: Theory, simulations, experiments

F. Roters, P. Eisenlohr, L. Hantcherli, D.D. Tjahjanto, T.R. Bieler, D. Raabe: Acta Materialia 58 (2010) 1152–1211
Overview of constitutive laws, kinematics, homogenization and multiscale methods in crystal plasticity finite-element modeling: Theory, experiments, applications